GALAXY EVOLUTION IN THE ENVIRONMENT OF RDCS J1252.9-2927 AT $z \sim 1.24$ (II) - TANAKA CATALOG

NEDELIA ANTONIA POPESCU

Astronomical Institute of Romanian Academy
Str. Cutitul de Argint 5, 40557 Bucharest, Romania
Email: nedelia@aira.astro.ro

Abstract. In this paper we study the environment of RDCS J1252.9-2927, at $z = 1.237$, using the catalog of Tanaka *et al.*(2009) with optical-NIR photometric data and redshifts for 120 galaxies. The data from this catalog cover a wide field of 875 arcmin^2 (25 arcmin $\times$ 35 arcmin field), making possible the study of the large-scale structures in the field of RDCS J1252.9-2927 cluster. The color-color and color-magnitude diagrams of the galaxies that belong to the large-scale structures CLUMP 1 and CLUMP 2 in the RDCS J1252.9-2927 environment are presented. A large population of Extremely Red Galaxies (ERGs) in the studied sample of galaxies is determined. The photometric properties of galaxies in pairs and groups in the CLUMP 1 and CLUMP 2 are also analyzed.

Key words: galaxy groups and clusters - galaxy-galaxy interactions - galaxy pairs.

1. INTRODUCTION

The RDCS J1252.9-2927 cluster is one of the highest redshift X-ray clusters that was discovered in ROSAT Deep Cluster Survey (Rosati *et al.*, 2004). In the cosmological model $H_0 = 70$ km s^{-1} Mpc^{-1},$\Omega_m = 0.3$, $\Omega_\Lambda = 0.7$, $h = 0.7$, the total mass of the cluster inside 0.5 Mpc radius was estimated by Rosati *et al.* (2004) as being $M(< 0.5Mpc) = (1.9 \pm 0.3) \times M_\odot^{14}$.

In the same cosmological model, Lombardi *et al.* (2005) determined the total mass inside 1 Mpc radius to be $M(< 1Mpc) = (8 \pm 0.3) \times M_\odot^{14}$.

Blakeslee *et al.* (2003) reported the images obtained with the Advanced Camera for Surveys (ACS) on the Hubble Space Telescope (HST) in the F775W and F850LP bandpasses. A tight colour-magnitude relation (CMR) of early-type galaxies belonging to this cluster was revealed by these authors. In the core of the cluster a central pair of galaxies, with signs of dynamical interaction, surrounded by a large early-type galaxy population were determined due to the special resolution of ACS.

Lidman *et al.* (2004), Toft *et al.* (2004), and Strazzullo *et al.* (2006) obtained the ground-based near-IR imaging of RDCS J1252.9-2927 environment, underlying a clear near-IR color-magnitude relation (CMR). The luminosity function of the cluster galaxies was analyzed too, and a shallower slope than the value measured at similar

restframe wavelength in clusters in the local universe was revealed.

Due to a detailed dynamical and spectrophotometric information on galaxies in RDCS J1252.9-2927 high redshift cluster, Demarco *et al.* (2007) provided an in-depth view of structure formation at this epoch.

Tanaka *et al.* (2009) extended the investigation, obtaining wide-field imaging observations of the X-ray luminous cluster RDCS J1252.9-2927. Several galaxy groups that seem to be embedded in a filamentary structure extending from the cluster core are present inside the cluster.

Using GMOS on Gemini-South and FORS2 on VLT, Tanaka *et al.* (2009) performed a spectroscopic study of the galaxies in order to determine if these galaxies are physically associated to the cluster. The authors concluded that three groups contain galaxies at the cluster redshift, being probably bound to the cluster. The presence of such a filamentary structure as traced by galaxy groups at $z > 1$ was for the first time confirmed.

In the previous paper (Popescu, 2011) we combined the catalog of Demarco *et al.* (2007), that contains optical-NIR photometric data, redshifts, and morphology for galaxies (in a 36 arcmin^2 field), with Hubble Space Telescope/ Advanced Camera for Surveys archival images (from Hubble Space Telescope Archive at Canadian Astronomy Data Centre). The distribution of galaxies in the field of RDCS J1252.9-2927, taking into account their spectroscopic redshifts and morphology was analyzed. The role of color-color and color-magnitude diagrams in the characterization of Extremely Red Objects (EROs) was underlined. The photometric and morphological properties of galaxies in pairs and groups in the RDCS J1252.9-2927 environment were also determined. We especially consider the role of galaxy-galaxy interactions in triggering the star formation, and strong modification of galaxy morphologies and colors.

In this paper we study the environment of RDCS J1252.9-2927, at $z = 1.237$, using the catalog of Tanaka *et al.* (2009) with optical-NIR photometric data and redshifts for 120 galaxies.

The data from this catalog cover a large field of 875 arcmin^2 (25 arcmin $\times$ 35 arcmin field), making possible the study of the large-scale structures in the field of RDCS J1252.9-2927.

The color-color and color-magnitude diagrams of the galaxies that belong to the large-scale structures CLUMP 1 and CLUMP 2 in the RDCS J1252.9-2927 environment are presented. The photometric properties of galaxies in pairs and groups in the CLUMP 1 and CLUMP 2 are also analyzed.

2. DISTRIBUTION OF GALAXIES - TANAKA CATALOG

In the cosmological model $H_0 = 70$ km s^{-1} Mpc^{-1},$\Omega_m = 0.3$, and $\Omega_\Lambda = 0.7$, at the cluster redshift of $z = 1.237$, a linear size of 0.5 Mpc corresponds to $1'$ on the sky (*i.e.* $1''$ on the sky corresponds to 8.33 kpc in a physical distance).

Fig.1 presents the 2D distribution of galaxies in the RDCS J1252.9-2927 field for:

- the catalog of Demarco *et al.* (2007), with (B, V, R, $i775$, $z850$, K) optical-NIR photometric data, redshifts, and morphology for 38 confirmed cluster galaxies and redshifts for 189 field galaxies (in a 36 arcmin^2 field)- see Popescu (2011);

- the catalog of Tanaka *et al.* (2009), with (V, R, i', z', Ks) optical-NIR photometric data and redshifts for 120 galaxies positioned in CLUMP 1, CLUMP 2, CLUMP 3 and CLUMP 4 (in a 875 arcmin^2 field).

In both catalogs the magnitudes are on the AB system (Oke, 1974), being corrected for Galactic extinction.

Tanaka *et al.* (2007) observed RDCS J1252.9-2927 with Suprime-Cam (Miyazaki *et al.* , 2002) on the Subaru Telescope in the (V, R, i', z') bands, and K-band imaging with WFCAM on UKIRT (Henry *et al.* , 2000) and K_s-band imaging with SOFI on the ESO NTT (Moorwood, Cuby, and Lidman, 1998). In Tanaka *et al.* (2007) were for the first time presented four poor groups around the RDCS J1252.9-2927 cluster at $z \sim 1.24$.

In order to obtain spectroscopic follow-up observations of the structures discovered in Tanaka *et al.* (2007), Tanaka *et al.* (2009) used GMOS on Gemini-South (Hook *et al.* , 2004) and FORS2 on VLT UT1 (Appenzeller *et al.* , 1998). The catalog obtained by Tanaka *et al.* (2009) contains 102 objects with secure redshifts and 18 objects with possible redshifts.

In Fig.1, the RDCS J1252.9-2927 cluster can be clearly identified at the centre of the field, containing 38 confirmed cluster galaxies (big dots) and 189 field galaxies (small dots). In this figure North is up and Est is to the right. The distribution of $z \sim 1.24$ galaxies presents clumpy structures that surround the central main cluster. It can be observed the presence of a chain of clumps towards the N-NE direction from the cluster RDCS J1252.9-2927, reprezented by the CLUMP 1 and CLUMP 2, and extending over 15 Mpc transverse comoving distance. At the E-NE and W-SW of the main cluster a few more clumps are present. The CLUMP 3 and CLUMP 4 are located at E-NE of the main cluster, and W-SW of the main cluster, respectively. A large filamentary structure extending about 20 Mpc transverse comoving distance in the NE-SW direction is present.

The 3D distribution of the galaxies in the RDCS J1252.9-2927 cluster field function of the position (X,Y) and the spectroscopic redshifts z is presented in Fig.2.

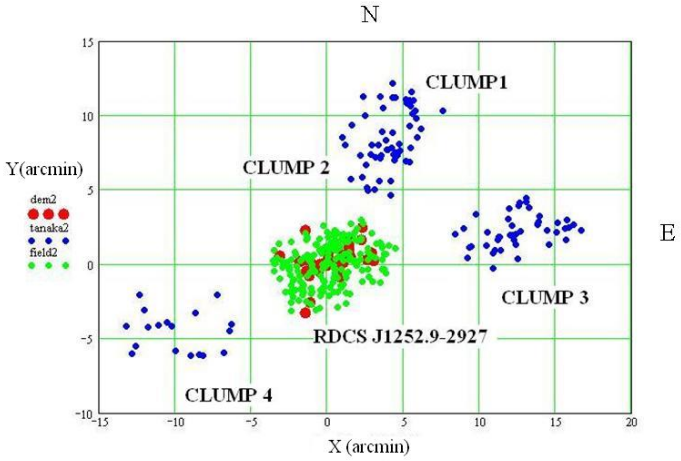

Fig. 1 – The 2D distribution of the galaxies in the RDCS J1252.9-2927 cluster field.

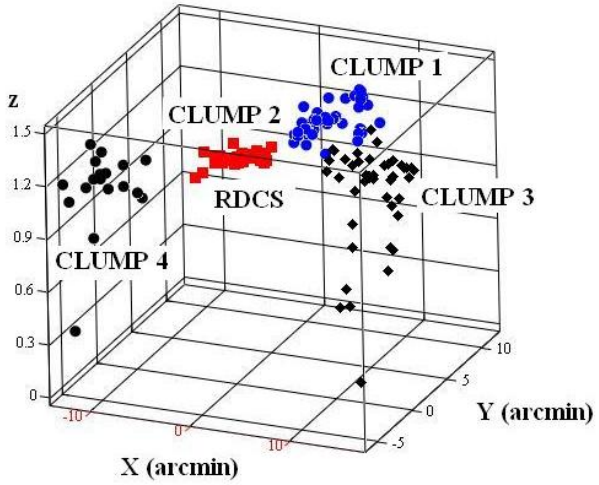

Fig. 2 – The 3D distribution of the galaxies in the RDCS J1252.9-2927 cluster field as function of the position (X,Y) and the spectroscopic redshifts z.

3. COLOR-MAGNITUDE AND COLOR-COLOR DIAGRAMS OF THE GALAXIES IN CLUMP 1 AND CLUMP 2

Elston *et al.* (1988) first discovered a special population denoted extremely red objects (EROs). These objects are characterized by very red optical and near-infrared colors, and are difficult to be classified due to their faintness. Extremely Red Galaxies (ERGs) are a subset of EROs, and are considered to be a mixture of mainly

two different populations at redshifts higher than $z = 1$.

The red colors of ERGs population are consistent with the following two classes of galaxies:

i) passively evolving early-type galaxies (elliptical and S0) in the redshift range $1 < z < 2$;

ii) high-redshift dusty starburst galaxies (characterized by high star-formation rates) whose UV luminosities are strongly absorbed by internal dust, or AGN reddened by strong dust extinction.

For the identification of galaxies clusters at $z \geq 1$, the selection criteria of the passively evolving elliptical galaxies by means of red optical and near-infrared colors have been usually used. Because the 4000 $\dot{A}$ break falls between R- (or I-, J-) band and K band, at $z \geq 1$ old passively-evolving galaxies should be characterized by red optical-NIR colors, which are redder than most galactic stars and field galaxies colors.

Both galaxy populations mentioned above satisfy color thresholds for ERGs such as $(R-K)_{Vega} \geq 5$, $(I-K)_{Vega} \geq 4$, $(V-I)_{Vega} \geq 3.5$, and have moderately faint near-infrared magnitudes ($K \sim 17.5-20$). These two populations can be separated by their morphology, spectra or color. Using the color-color diagrams, $(R-K)$ vs $(J-K)$ colors, Mannucci *et al.* (2002) have separated the two populations, and have found that the two populations have similar abundances in their 57 ERGs sample.

To analyze the ERGs in the Tanaka catalogue, we have to transform the photometry from the AB system to the Vega-based system using Fukugita, Shimasaku and Ichikawa (1995) transformations. The AB magnitudes and Vega-based magnitudes are denoted with (AB) and (Vega), respectively.

In our analysis the following transformation formulae from AB magnitudes to Vega-based magnitudes are considered:

$$V_{Vega} = V_{AB} - 0.011; R_{Vega} = R_{AB} - 0.199 \quad (1)$$

$$i'_{Vega} = i'_{AB} - 0.401; z'_{Vega} = z'_{AB} - 0.549 \quad (2)$$

For K magnitude the scales between the Vega-based magnitudes and the AB magnitudes are given by the formulae (Miyazaki *et al.* , 2003):

$$Ks_{Vega} = Ks_{AB} - 1.8 \quad (3)$$

$$(R-Ks)_{Vega} = (R-Ks)_{AB} + 1.6 \quad (4)$$

In this paper we define ERGs as objects whose color is equal to or redder than 3.4 (*i.e.* the condition $(R-Ks)_{AB} \geq 3.4$). This is the equivalent of the usual definition relation $(R-K)_{Vega} \geq 5$.

Because the goal of this paper is to analyze the ERGs distribution and the interactions effects on galaxies colors, in the sequel we analyze the color distribution of the galaxies that belong to CLUMP 1 and CLUMP 2 together (these two clumps being positioned very close to one another).

Fig.3 presents the 2D distribution of galaxies in CLUMP 1 and CLUMP 2, function of the spectroscopic redshifts z. From the 58 galaxies that belong to CLUMP 1 and CLUMP 2, in Fig.3 are represented 46 galaxies as follows: big dots - 18 galaxies with $z = 1.234$; diamonds - 5 galaxies with $z = 1.21$; (+) - 11 galaxies with $1.18 < z < 1.198$; small dots - 12 galaxies with $z = 1.1$. With big squares are marked the 15 galaxies that belong to the sample of galaxies pairs from CLUMP 1 and CLUMP 2.

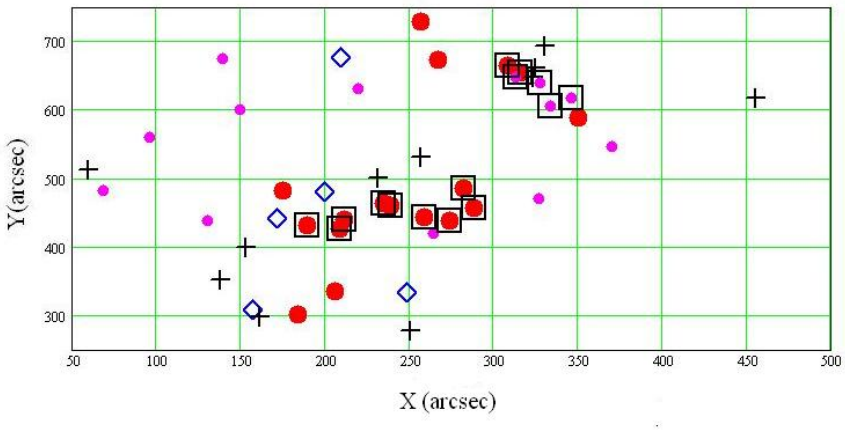

Fig. 3 – The 2D distribution of the galaxies in the CLUMP 1 and CLUMP 2 function of the spectroscopic redshifts z. The symbols are as follows: big dots - 18 galaxies with $z = 1.234$; diamonds - 5 galaxies with $z = 1.21$; (+) - 11 galaxies with $1.18 < z < 1.198$; small dots - 12 galaxies with $z = 1.1$.

The color-magnitude diagrams $(R-Ks)_{AB} - K_{AB}$, $(i'-Ks)_{AB} - K_{AB}$ and color-color diagram $(R-Ks)_{AB} - (i'-Ks)_{AB}$ of galaxies function of the spectroscopic redshifts z are presented in Fig.4. The symbols in Fig.4 are the same as in Fig.3. The dashed horizontal line in Fig.4 (top panel) represents the threshold $(R-Ks)_{AB} = 3.4$ for the selection of ERGs. In Fig.4 (middle panel) the two dashed horizontal lines represent the boundaries $(i'-Ks)_{AB} = 2.5$ and $(i'-Ks)_{AB} = 3.5$ for the galaxies in the red sequence. The vertical line represents the separation line between red and blue galaxies for $(i'-K)_{AB} = 2.5$, in Fig.4 (bottom panel).

The presence of a large population of ERGs in the CLUMP 1 and CLUMP 2 from the Catalog of Tanaka *et al.* (2009) is revealed by the color-color diagram

$(R-Ks)_{AB}-(i'-Ks)_{AB}$. The clustering of the 14 ERGs in specific colors ranges is obvious. The concentrations of red galaxies in the two clumps strongly suggest that these clumps are physically bound systems.

The color-color diagram $(V-i')_{AB}-(i'-z)_{AB}$, presented in Fig.5, is useful for the selection of Balmer/4000 $\dot{A}$ break galaxies and star-forming galaxies applying the selection criteria (Demarco *et al.* , 2007):

$$0.4 < (i'-z)_{AB} < 0.87; 0.2 < (V-i')_{AB} < 1.2 \quad (5)$$

$$2.4(i'-z)_{AB} - 1.12 < (V-i')_{AB} < 7(i'-z)_{AB} - 2.3 \quad (6)$$

The two population of old passive evolving galaxies and star-forming galaxies are well delimited in the $(R-Ks)_{AB}-(i'-Ks)_{AB}$ (Fig.4, bottom panel) and $(V-i')_{AB}-(i'-z)_{AB}$ (Fig.5) color-color diagrams. The red galaxies have colors in the specific range of the old passively evolving galaxies at $z \sim 1$. The condition $2.5 < (i'-Ks)_{AB} < 3.5$ is broad enough to include galaxies from the color-magnitude diagram in the red sequence. Also, the red sequence of studied galaxies is well delimited in the color-magnitude diagram $(R-Ks)_{AB}-Ks_{AB}$ from Fig.4 (top panel).

4. THE GALAXY PAIRS SAMPLE

To select kinematic galaxy pairs, in our study three steps are followed:

(1) For each galaxy in the spectroscopic redshift sample are determined the kinematic companions with a relative line-of-sight velocity difference $|\Delta v| \leq 500$ km s^{-1} and a projected physical separation (onto the plane of the sky) $r_{proj} \leq 300$ h^{-1} kpc.

(2) In the selected kinematic companions sample, close pairs are considered if they satisfy 10 h^{-1} kpc $\leq r_{proj} \leq 50$ h^{-1} kpc (Lin *et al.* , 2007; Patton and Atfield 2008; Patton *et al.* , 2011).

(3) Wide pairs are identified as kinematic companions with 50 h^{-1}kpc $\leq r_p \leq$ 300 h^{-1} kpc.

The linear distance between two galaxies can be obtained using the projected separation:

$$r_{proj} = \theta d_A(z_P). \quad (7)$$

The rest-frame relative velocity along the line of sight is determined as:

$$\Delta v = c|z_C - z_P|/(1+z_P). \quad (8)$$

In these formulae z_P is the redshift of the principal (more luminous) galaxy in the pair; z_C is the redshift of the companion galaxy; θ is the angular separation of the

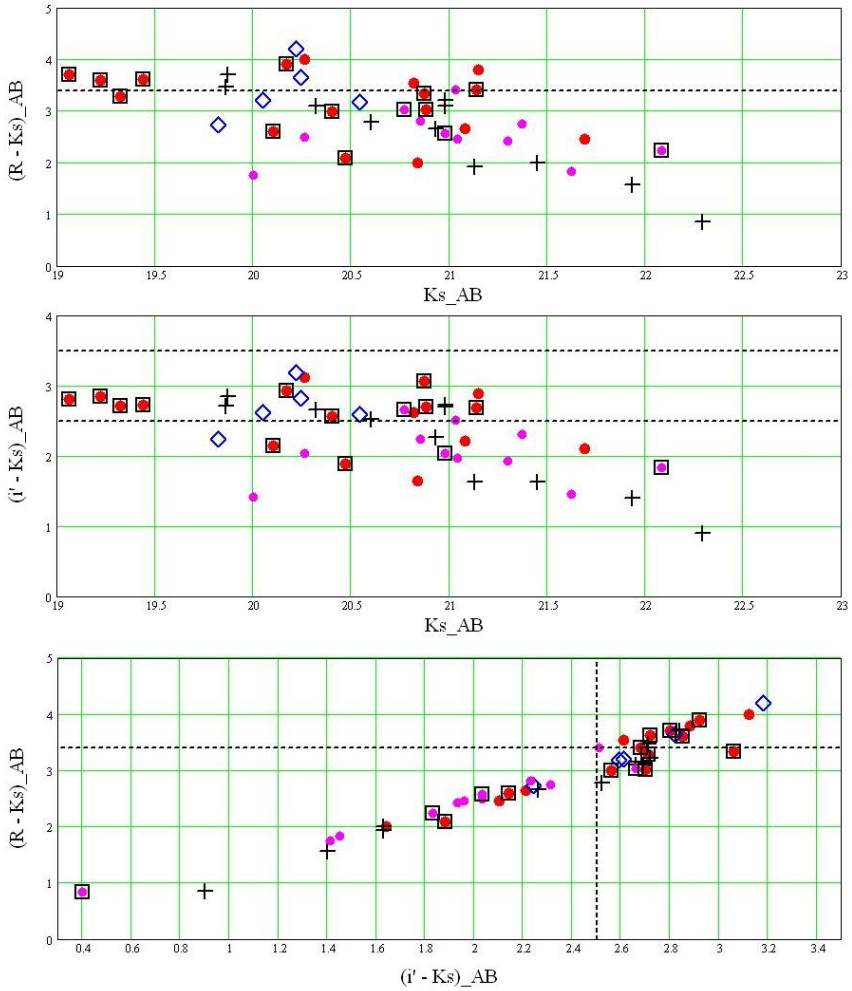

Fig. 4 – The $(R-Ks)_{AB}-Ks_{AB}$ color-magnitude diagram(top panel); $(i'-Ks)_{AB}-Ks_{AB}$ color-magnitude diagram (middle panel); $(R-Ks)_{AB}-(i'-Ks_{AB})$ color-color diagram (bottom panel); The symbols are as follows: big dots - 18 galaxies with $z\sim 1.234$; diamonds - 5 galaxies with $z=1.21$; (+) - 11 galaxies with $1.18<z<1.198$; small dots - 12 galaxies with $z=1.1$.

two galaxies on the sky plane (in arcsec); $d_A(z)$ is the angular scale at redshift z (in kpc/arcsec).

Because for the 46 galaxies in CLUMP 1 and CLUMP 2 secure redshifts are available, in the selection of our galaxy pairs sample we have the redshifts for both members of a pair. In this way the contamination due to unrelated foreground/ background companions is excluded, and we can compare intrinsic galaxy properties as a

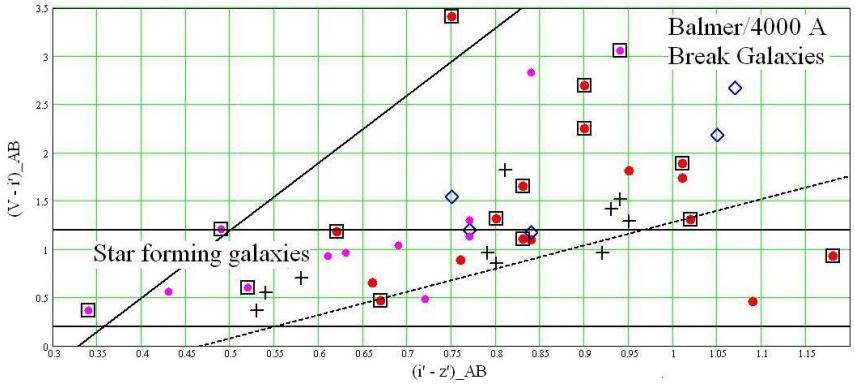

Fig. 5 – The $(V - i')_{AB} - (i' - z)_{AB}$ color-color diagram.

function of projected physical separation and relative line-of-sight velocity.

In Table 1 the photometric characteristics of the 15 galaxies in the galaxy pairs sample are described. We observe that the galaxies in pairs present obvious features of interactions, with bluer $(V - i')_{AB}$ and $(i' - z')_{AB}$ colors, as characteristics of interactions/mergers that trigger star formation activity.

Among the 15 galaxies that form 5 pairs and 2 triplets, only the pair formed by galaxies with identification number ID13 and ID15 has the projected distance less than 50 h^{-1}kpc, being a close pair of galaxies. The other galaxies represent wide pairs o galaxies, with projected distances in the range 100 h^{-1}kpc $\leq r_p \leq$ 270 h^{-1} kpc.

5. THE EFFECTS OF INTERACTIONS/MERGERS ON GALAXIES COLORS

Because of the different procedures for defining samples of galaxy pairs, the determined mergers present different properties.

Concluding, there are two main ways to define samples of mergers:

1) Based on morphological criteria - this procedure is focused on structural disturbances and/or tidal features (Bridge *et al.* , 2010; Chou *et al.* , 2011). Mergers tend to present strong morphological disturbances at the first encounter and the last merging stage. Then, the morphological selection criteria are biased toward selecting mergers at the final merging stages.

2) Based on a kinematic selection - this procedure identifies mergers by limiting the projected physical separation and the velocity differences between two close pair members (Patton *et al.* , 2000; Lin *et al.* , 2008; Patton and Atfield , 2008; Patton *et al.* , 2011).

In our study we used the kinematic selection in the detection of the galaxy

Table 1

The photometric characteristics of galaxy pairs sample

ID	K_{AB}	z_{spec}	$(R-Ks)_{AB}$	$(i'-Ks)_{AB}$	$(V-i')_{AB}$	$(i'-z')_{AB}$
5	19.06	1.235	3.70	2.80	2.70	0.90
6	20.17	1.237	3.90	2.92	2.25	0.90
19	20.88	1.234	3.02	2.70	3.41	0.75
17	20.87	1.226	3.34	3.06	0.93	1.18
22	21.14	1.231	3.41	2.68	1.31	1.02
13	20.40	1.231	2.99	2.56	1.11	0.83
15	19.32	1.235	3.29	2.71	1.32	0.80
18	19.22	1.233	3.60	2.85	1.89	1.01
21	20.10	1.234	2.60	2.14	1.18	0.62
14	19.44	1.235	3.62	2.72	1.65	0.83
14	19.44	1.235	3.62	2.72	1.65	0.83
47	20.47	1.231	2.09	1.88	0.47	0.67
2	22.08	1.068	2.23	1.83	0.60	0.52
1	24.63	1.071	0.83	0.40	0.37	0.34
8	20.77	1.070	3.03	2.66	3.06	0.94
9	20.98	1.070	2.57	2.03	1.21	0.49

mergers sample, as was presented in the previous section.

In order to investigate the interactions/mergers effects on galaxy colors, in Fig.6 the color-magnitude diagram $(R-Ks)_{AB}-K_{AB}$ and color-color diagram $(R-Ks)_{AB}-(i'-Ks)_{AB}$ for the 15 galaxies in pairs are presented.

In Fig.7 is displayed the color-color diagram $(V-i')_{AB}-(i'-z)_{AB}$ for the studied pairs of galaxies. This diagram is useful for the selection of Balmer/4000 $\dot{A}$ break galaxies and star-forming galaxies applying the selection criteria of Demarco *et al.* (2007).

In Figs. 6 and 7, the galaxies in pairs are represented with: big dots (ID5 and ID6 galaxies); diamonds (ID19, ID17, ID22 galaxies); crosses (ID13, ID15 galaxies); (X) (ID18, ID21, ID14 galaxies); squares (ID14, ID47 galaxies); small diamonds (ID1, ID2 galaxies); small dots (ID8, ID9 galaxies).

Clear evidences of interaction-induced star formation within the blue galaxies in pairs is revealed by Fig.7. Here a higher fraction of extremely blue galaxies are positioned in the *star forming galaxy region*. Also, the presence of red-red pair (candidate for dry merger), blue-blue pair (candidate for wet merger), and red-blue pair (candidate for mixed pair) in the determined sample of galaxy pairs can be observed in Fig.7. The wet mergers refer to galaxy mergers between gas-rich galaxies (*i.e.* mergers between galaxies with intense star formation), while dry mergers are those mergers between gas-poor galaxies (*i.e.* mergers between elliptical/spheroidal galaxies, that have weak star formation).

We classify as red fraction, the fraction of galaxies that either belong to the red

sequence or to the ERGs population (extremely red galaxies).

In the case of the galaxy pair sample from CLUMP 1 and CLUMP 2, one observes that the majority of blue-blue pairs are found in field-like environments. Also, red-red pairs and blue-red pairs tend to lie in denser environments (group and/or cluster-like environments), as can be seen from Fig.3 and Table 1 inspection.

The group of galaxies with $z \sim 1.24$ contains mainly red-red pairs and 3 mixed red-blue pairs, as can be observed from Table 1.

The only close pair of galaxy (ID13, ID15), with $r_p = 41.5$ kpc, belonging to the group of galaxies with $z \sim 1.24$, has the photometric characteristics:
- ID2 galaxy: K_{AB}=20.40, $(R-Ks)_{AB}$=2.99, $(i'-Ks)_{AB}$=2.56, $(V-i')_{AB}$=1.11, $(i'-z')_{AB}$= 0.83;
- ID1 galaxy: K_{AB}=19.32, $(R-Ks)_{AB}$=3.29, $(i'-Ks)_{AB}$=2.71, $(V-i')_{AB}$=1.32, $(i'-z')_{AB}$= 0.80.

The clump of galaxies with $z \sim 1.1$ contains only 2 galaxy pairs that present the most bluer colors in the sample. These pairs are positioned in a field-like environment.

The blue - blue pair (ID2, ID1) has a projected distance $r_p = 132$ kpc and the photometric characteristics:
- ID2 galaxy: K_{AB}=22.08, $(R-Ks)_{AB}$=2.23, $(i'-Ks)_{AB}$=1.83, $(V-i')_{AB}$=0.70, $(i'-z')_{AB}$= 0.52;
- ID1 galaxy: K_{AB}=24.63, $(R-Ks)_{AB}$=0.83, $(i'-Ks)_{AB}$=0.40, $(V-i')_{AB}$=0.37, $(i'-z')_{AB}$= 0.34.

This galaxy pair contains the faintest and bluest galaxies in the sample of 46 galaxies from CLUMP 1 and CLUMP 2.

The red - blue pair (ID8, ID9) has the photometric characteristics:
- ID8 galaxy: K_{AB}=20.77, $(R-Ks)_{AB}$=3.03, $(i'-Ks)_{AB}$=2.66, $(V-i')_{AB}$=3.06, $(i'-z')_{AB}$= 0.94;
- ID9 galaxy: K_{AB}=20.98, $(R-Ks)_{AB}$=2.57, $(i'-Ks)_{AB}$=2.03, $(V-i')_{AB}$=1.21, $(i'-z')_{AB}$= 0.49.

The wet and dry merging populations show different evolutionary trends. In their recent studies, Lin *et al.* (2008), De Propris *et al.* (2010), and Chou *et al.* (2011) show that the fraction of dry mergers (from the total merging galaxy population) is low at high redshifts (at $z > 0.5$), but becomes important at low redshifts ($z < 0.2$).

6. CONCLUSIONS

In this paper we study the environment of RDCS J1252.9-2927, at $z = 1.237$, using the catalog of Tanaka *et al.* (2009) with optical-NIR photometric data and

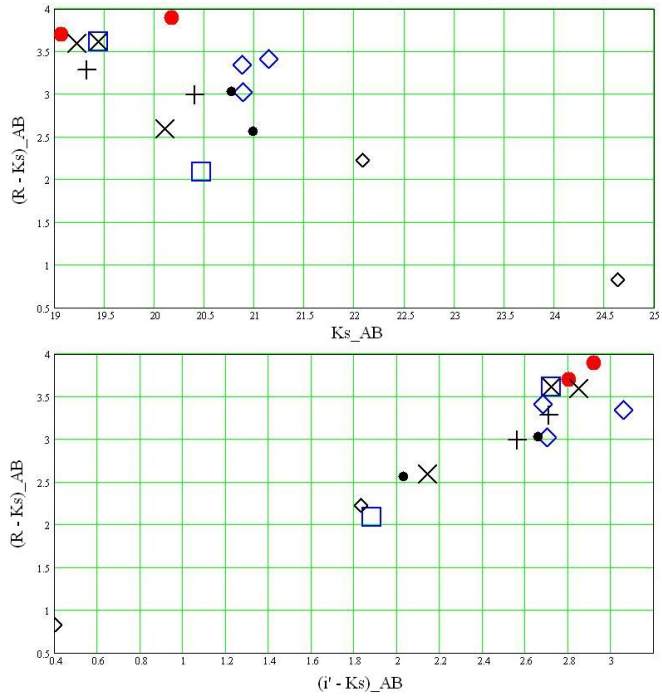

Fig. 6 – The $(R-Ks)_{AB} - Ks_{AB}$ color-magnitude diagram for the galaxy pair sample (top panel) and $(R-Ks)_{AB} - (i' - Ks_{AB})$ color-color diagram (bottom panel).
The symbols are as follows: big dots (ID5 and ID6 galaxies); diamonds (ID19, ID17, ID22 galaxies); crosses (ID13, ID15 galaxies); (X) (ID18, ID21, ID14 galaxies); squares (ID14, ID47 galaxies); small diamonds (ID1, ID2 galaxies); small dots (ID8, ID9 galaxies).

redshifts for 120 galaxies. The data from this catalog cover a wide field of 875 arcmin^2 (25 arcmin $\times$ 35 arcmin field).

In the field of RDCS J1252.9-2927, the distribution of galaxies presents 4 clumpy structures that surround the central main cluster. A large filamentary structure extending about ~ 20 Mpc in the NE-SW direction is present. Because of the concentrations of red galaxies in the clumps, it is strongly suggested that these are physically bound systems.

The color-color and color-magnitude diagrams of the galaxies that belong to the large-scale structures CLUMP 1 and CLUMP 2 in the RDCS J1252.9-2927 environment are presented. By means of these diagrams, a large population of 14 Extremely Red Galaxies (ERGs) is determined.

A strong pair isolation criterion in terms of the apparent angular separation and rest-frame line-of-sight velocity difference is used to obtain the galaxy pairs sample. The photometric properties of galaxies in pairs and triplets in CLUMP 1 and CLUMP

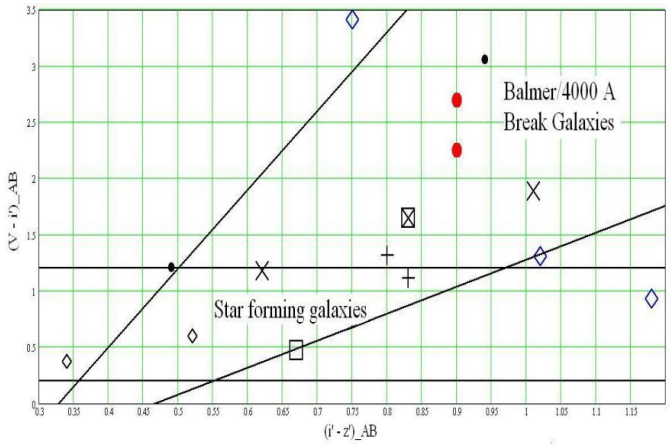

Fig. 7 – The $(V - i')_{AB} - (i' - z)_{AB}$ color-color diagram for the galaxy pair sample. The symbols are as follows: big dots (ID5 and ID6 galaxies); diamonds (ID19, ID17, ID22 galaxies); crosses (ID13, ID15 galaxies); (X) (ID18, ID21, ID14 galaxies); squares (ID14, ID47 galaxies); small diamonds (ID1, ID2 galaxies); small dots (ID8, ID9 galaxies).

2 are also analyzed. A large fraction of red galaxies in pairs or triplets is determined (11 red galaxies from the 15 galaxies in pairs). The redder colours are due to the higher densities of galaxies (especially for CLUMP 2) and the fact that galaxy colour and local density are correlated. The bluer optical-NIR colors of galaxies is a result of an increased star formation rate due to possible interactions/mergers.

REFERENCES

Appenzeller, I., Fricke, K., Fürtig, W., Gässler, W., Häfner, R., Harke, R., Hess, H.-J., Hummel, W., Jürgens, P., Kudritzki, R.-P., Mantel, K.-H., Meisl, W., Muschielok, B., Nicklas, H., Rupprecht, G., Seifert, W., Stahl, O., Szeifert, T., and Tarantik, K.: 1998, *The Messenger* **94**, 1.

Blakeslee, J.P., Franx, M., Postman, M., Rosati, P., Holden, B.P., Illingworth, G.D., Ford, H.C., Cross, N.J.G., Gronwall, C., Benítez, N., Bouwens, R.J., Broadhurst, T.J., Clampin, M., Demarco, R., Golimowski, D.A., Hartig, G.F., Infante, L., Martel, A.R., Miley, G.K., Menanteau, F., Meurer, G.R., Sirianni, M., and White, R.L.: 2003, *Astrophys. J.* **596**, L143.

Bridge, C.R., Carlberg, R.G., and Sullivan, M.: 2010, *Astrophys. J.* **709**, 1067.

Chou, R.C.Y., Bridge, C.R., and Abraham, R.G.: 2011, *Astron. J.* **141**, 87.

Demarco, R., Rosati, P., Lidman, C., Girardi, M., Nonino, M., Rettura, A., Strazzullo, V., van der Wel, A., Ford, H.C., Mainieri, V., Holden, B.P., Stanford, S.A., Blakeslee, J.P., Gobat, R., Postman, M., Tozzi, P., Overzier, R.A., Zirm, A.W., Benítez, N., Homeier, N.L., Illingworth, G.D., Infante, L., Jee, M.J., Mei, S., Menanteau, F., Motta, V., Zheng, W., Clampin, M., and Hartig, G.: 2007, *Astrophys. J.* **663**, 164.

De Propris, R., Driver, S.P., Colless, M., Drinkwater, M.J., Loveday, J., Ross, N.P., Bland-Hawthorn, J., York, D.G., and Pimbblet, K.: 2010, *Astron. J.* **139**, 794.

Fukugita, M., Shimasaku, K., and Ichikawa, T.: 1995, *Pub. Astron. Soc. Pac.* **107**, 945.

Henry, D.M., Atad-Ettedgui, E., Casali, M.M., Bennett, R.J., Bridger, A., Ives, D.J., Rae, R.G., and

Hawarden, T.G.: 2000, *Society of Photo-Optical Instrumentation Engineers (SPIE) Conference Series* **4008**, 1325.

Hook, I.M., Jørgensen, I., Allington-Smith, J.R., Davies, R.L., Metcalfe, N., Murowinski, R.G., and Crampton, D.: 2004, *Pub. Astron. Soc. Pac.* **116**, 425.

Lidman, C., Rosati, P., Demarco, R., Nonino, M., Mainieri, V., Stanford, S.A., and Toft, S.: 2004, *Astron. Astrophys.* **416**, 829.

Lin, L., Koo, D.C., Weiner, B.J., Chiueh, T., Coil, A.L., Lotz, J., Conselice, C.J., Willner, S.P., Smith, H.A., Guhathakurta, P., Huang, J.-S., Le Floc'h, E., Noeske, K.G., Willmer, C.N.A., Cooper, M.C., and Phillips, A.C.: 2007, *Astrophys. J.* **660**, L51.

Lin, L., Patton, D.R., Koo, D.C., Casteels, K., Conselice, C.J., Faber, S.M., Lotz, J., Willmer, C.N.A., Hsieh, B.C., Chiueh, T., Newman, J.A., Novak, G.S., Weiner, B.J., and Cooper, M.C.: 2008, *Astrophys. J.* **681**, 232.

Lombardi, M., Rosati, P., Blakeslee, J.P., Ettori, S., Demarco, R., Ford, H.C., Illingworth, G.D., Clampin, M., Hartig, G.F., Benítez, N., Broadhurst, T.J., Franx, M., Jee, M.J., Postman, M., and White, R.L.: 2005, *Astrophys. J.* **623**, 42.

Mannucci, F., Pozzetti, L., Thompson, D., Oliva, E., Baffa, C., Comoretto, G., Gennari, S., and Lisi, F.: 2002, *Mon. Not. Roy. Astron. Soc.* **329**, L57.

Miyazaki, S., Komiyama, Y., Sekiguchi, M., Okamura, S., Doi, M., Furusawa, H., Hamabe, M., Imi, K., Kimura, M., Nakata, F., Okada, N., Ouchi, M., Shimasaku, K., Yagi, M., and Yasuda, N.: 2002, *Pub. Astron. Soc. Japan* **54**, 833.

Miyazaki, M., Shimasaku, K., Kodama, T., Okamura, S., Furusawa, H., Ouchi, M., Nakata, F., Doi, M., Hamabe, M., Kimura, M., Komiyama, Y., Miyazaki, S., Nagashima, C., Nagata, T., Nagayama, T., Nakajima, Y., Nakaya, H., Pickles, A.J., Sato, S., Sekiguchi, K., Sekiguchi, M., Sugitani, K., Takata, T., Tamura, M., Yagi, M., and Yasuda, N.: 2003, *Pub. Astron. Soc. Japan* **55**, 1079.

Moorwood, A., Cuby, J.-G., and Lidman, C.: 1998, *The Messenger* **91**, 9.

Oke, J.B.: 1974, *Astrophys. J. Suppl.* **27**, 21.

Patton, D.R., Carlberg, R.G., Marzke, R.O., Pritchet, C.J., da Costa, L.N., and Pellegrini, P.S.: 2000, *Astrophys. J.* **536**, 153.

Patton, D.R., and Atfield, J.E.: 2008, *Astrophys. J.* **685**, 235.

Patton, D.R., Ellison, S.L., Simard, L., McConnachie, A.W., and Mendel, J.T.: 2011, *Mon. Not. Roy. Astron. Soc.* **412**, 591.

Popescu, N.A.: 2011, *Romanian Astron. J.* **21**, 3.

Rosati, P., Tozzi, P., Ettori, S., Mainieri, V., Demarco, R., Stanford, S.A., Lidman, C., Nonino, M., Borgani, S., Della Ceca, R., Eisenhardt, P., Holden, B.P., and Norman, C.: 2004, *Astron. J.* **127**, 230.

Strazzullo, V., Rosati, P., Stanford, S.A., Lidman, C., Nonino, M., Demarco, R., Eisenhardt, P.E., Ettori, S., Mainieri, V., and Toft, S.: 2006, *Astron. Astrophys.* **450**, 909.

Toft, S., Mainieri, V., Rosati, P., Lidman, C., Demarco, R., Nonino, M., and Stanford, S.A.: 2004, *Astron. Astrophys.* **422**, 29.

Tanaka, M., Kodama, T., Kajisawa, M., Bower, R., Demarco, R., Finoguenov, A., Lidman, C., and Rosati, P.: 2007, *Mon. Not. Roy. Astron. Soc.* **377**, 1206.

Tanaka, M., Lidman, C., Bower, R.G., Demarco, R., Finoguenov, A., Kodama, T., Nakata, F., and Rosati, P.: 2009, *Astron. Astrophys.* **507**, 671.

Received on 5 October 2012